Phase diagram of mixed $Cu(In_xCr_{1-x})P_2S_6$ crystals

A. Dziaugys,[1,*] V. V. Shvartsman,[2,†] J. Macutkevic,[1] J. Banys,[1] Yu. Vysochanskii,[3] and W. Kleemann[2]
[1]*Faculty of Physics, Vilnius University, Sauletekio 9, Vilnius LT-10222, Lithuania*
[2]*Angewandte Physik, Universitat Duisburg-Essen, D-47048 Duisburg, Germany*
[3]*Institute of Solid State Physics and Chemistry of Uzhgorod University, Ukraine*
(Received 1 December 2011; revised manuscript received 23 January 2012; published 16 April 2012)

Mixed $Cu(In_xCr_{1-x})P_2S_6$ crystals of ferrielectric $CuInP_2S_6$ and antiferroelectric $CuCrP_2S_6$ were investigated by means of broadband dielectric spectroscopy (10 mHz–3 GHz), for several values of x. The phase boundary between the ferrielectric phase and the dipolar glass state was found to lie between 0.5 and 0.7, and a similar boundary between the dipolar glass state and the antiferroelectric phase is observed to be located between 0.4 and 0.2. The dipole freezing results in a broad distribution of the relaxation times. The parameters of the double-well potentials, the local polarization distribution function, and glass order parameter have been extracted from the dielectric measurements. From these results the complete phase diagram has been constructed.

DOI: 10.1103/PhysRevB.85.134105 PACS number(s): 77.80.−e, 77.22.Gm

I. INTRODUCTION

The nature of the dipolar glass phase is a puzzling problem in solid state physics. The main question concerns the very existence of a phase transition in dipolar glasses.[1] If there exists some phase transition, which kind of order parameter can describe it? At which temperature does the phase transition occur? A single order parameter splits into an array of the order parameters close to the glass transition temperature T_G for DRADP glasses.[2] However, the situation in betaine phosphite betaine phosphate (BP/BPI) dipolar glasses is more complicated.[3,4] From BP/BPI dielectric analysis follows that the nonzero average local potential asymmetry vanishes at very low temperatures, and this vanishing indicates the onset of a nonergodic dipolar glass phase.[4] Therefore, the freezing in BP/BPI dipolar glasses can be described by a single order parameter related to an average local potential asymmetry.

$CuInP_2S_6$ crystals represent an unusual example of a anticollinear two-sublattice ferrielectric system.[5–8] Here a first-order phase transition of order-disorder type from the paraelectric to the ferrielectric phase is realized ($T_c = 315$ K). The symmetry reduction at the phase transition ($C2/c \rightarrow Cc$) occurs due to ordering in the copper sublattice and displacement of cations in the indium sublattice from their centrosymmetric positions. The spontaneous polarization arising at the phase transition to the ferrielectric phase is perpendicular to the layer planes.

According to the results of calorimetric, dielectric, and x-ray diffraction measurements,[9,10] $CuCrP_2S_6$ undergoes a first-order phase transition into an antiferroelectric phase at $T_{C2} = 150$ K. At $T_{C1} = 190$ K this compound undergoes a second-order phase transition from the paraelectric ($T > T_{C1}$) to a quasi-antiferroelectric (incommensurate) phase ($T_{C2} < T < T_{C1}$). In this intermediate phase incomplete antipolar ordering of the copper was found.[11] $CuCrP_2S_6$ has $C2/c$ symmetry in the paraelectric and Pc in the antiferroelectric phase.[11]

These thiophosphates consist of lamellae defined by a sulfur framework, in which the metal cations and P-P pairs fill the octahedral voids; the Cu, In, Cr, and P-P ions form triangular patterns within the layer.[5–7] The cation off-centering, 1.6 for Cu^I and 0.2 Å for In^{III}, may be attributed to a second-order Jahn-Teller instability associated with the d^{10} electronic configuration. The lamellar matrix absorbs the structural deformations via the flexible P_2S_6 groups while restricting the cations to antiparallel displacements that minimize the energy costs of dipolar ordering. Each Cu^I ion can occupy two different positions. Relaxational rather than resonant behavior is indicated by the temperature dependence of the spectral characteristics in agreement with x-ray investigations. It was suggested that a coupling between P_2S_6 deformation modes and Cu^I vibrations enables the copper ion hopping motions that lead to the loss of polarity and the onset of ionic conductivity in this material at higher temperatures.[8] The investigation of ionic conductivity in $CuInP_2S_6$[12,13] has shown that σ_{DC} follows an Arrhenius law with the activation energy $E_A = 0.73$ eV,[12] while more detailed investigations showed $E_A = 0.635$ eV.[13] The activation energy of the ionic conductivity in $CuCrP_2S_6$ is very similar, viz. $E_A = 0.67$ eV.[12]

The magnetic properties of mixed $Cu(In_xCr_{1-x})P_2S_6$ were investigated in Ref. 14. The aim of this paper is to investigate the phase diagram of mixed $Cu(In_x\ Cr_{1-x})P_2S_6$ crystals via broadband dielectric spectroscopy.

II. EXPERIMENT

Crystals of $Cu(In_xCr_{1-x})P_2S_6$ were grown by the Bridgman method. For the dielectric spectroscopy polished platelike crystals were used. All measurements were performed in a direction perpendicular to the layers. Typical dimensions of samples were ≈10 mm^2 area and ≈0.1 mm thickness. The complex dielectric permittivity ε^* was measured using an HP4284A capacitance bridge in the frequency range 20 Hz to 1 MHz. In the frequency region from 1 MHz to 3 GHz measurements were performed by a coaxial dielectric spectrometer with a vector network analyzer Agilent 8714ET. The very low frequency dielectric measurements were carried out using a Solartron 1260 impedance analyzer with a 1296 dielectric interface. All measurements have been performed on cooling with controlled cooling rate of −0.25 K/min. Silver paste has been used for contacting.

III. RESULTS AND DISCUSSION

A. Ferrielectric phase transition in $Cu(In_xCr_{1-x})P_2S_6$ crystals

The temperature dependence of the dielectric permittivity of $CuInP_2S_6$ crystals with a small amount of chromium ($x = 0.8$) is presented in Fig. 1. A small amount of chromium significantly changes the dielectric properties of $CuInP_2S_6$ crystals: the temperature of the main dielectric anomaly shifts from about 315 to 245 K, the maximum value of the dielectric permittivity significantly decreases from about 180 to 45 at 10 MHz, at frequencies higher than about 10 MHz the peak of the dielectric permittivity becomes frequency dependent, and the critical slowing down disappears. An additional dielectric dispersion appears at low frequencies and at low temperatures. The additional low temperature dielectric dispersion is clearly expressed in the real part of complex dielectric permittivity, while the maximum of imaginary part of complex dielectric permittivity continuously decreases with frequency. The dielectric dispersion is related to dipolar glass behavior and denotes coexistence of ferroelectric order and dipolar glass disorder, similarly as in nominally pure $CuInP_2S_6$.[15] From Fig. 1 it can be seen that the dielectric permittivity at 50 kHz frequency and above the temperature 200 K already corresponds to the static one caused by the critical relaxation, because at that frequency and in this temperature range ε'' is already much smaller than ε'.

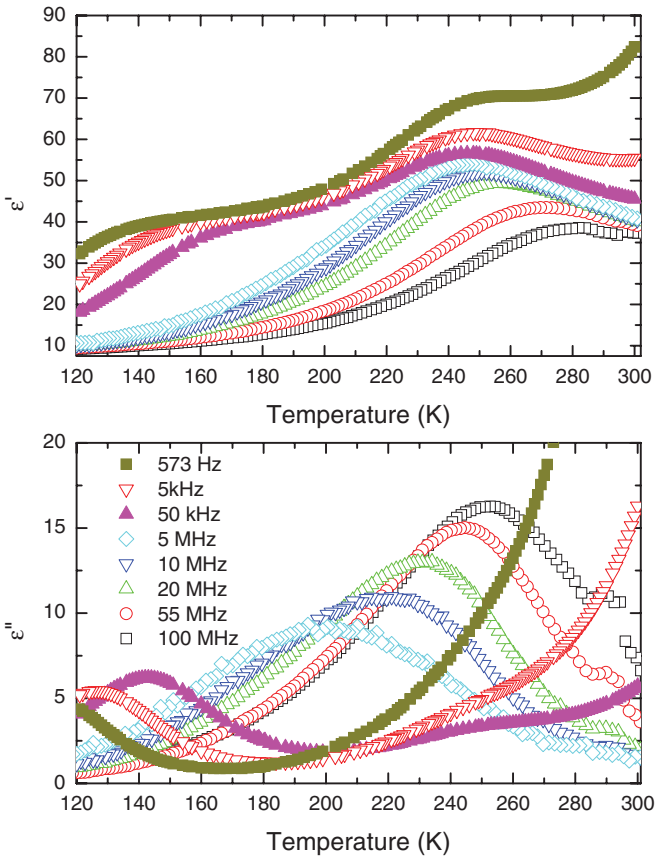

FIG. 1. (Color online) Temperature dependence of the complex dielectric permittivity of $Cu(In_{0.8}Cr_{0.2})P_2S_6$ crystals measured at several frequencies.

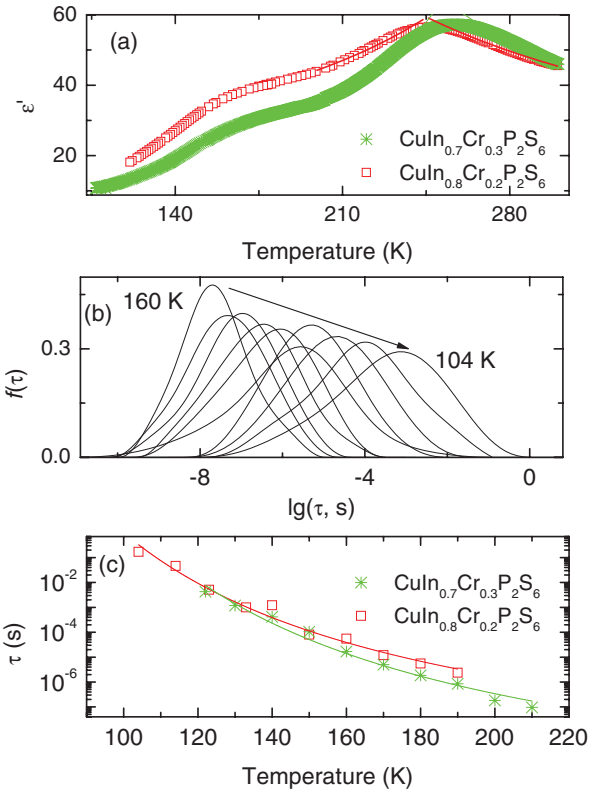

FIG. 2. (Color online) Temperature dependence of dielectric permittivity of $Cu(In_xCr_{1-x})P_2S_6$ ferrielectrics at 50 kHz (a); distribution of relaxation times of $Cu(In_{0.8}Cr_{0.2})P_2S_6$ (b); temperature dependence of longest relaxation times of $Cu(In_xCr_{1-x})P_2S_6$ ferrielectrics (c).

The peaks of the static dielectric permittivity close to $T = 256$ K for $CuIn_{0.7}Cr_{0.3}P_2S_6$ and close to $T = 240$ K for $CuIn_{0.8}Cr_{0.2}P_2S_6$ indicate ferroelectric phase transitions [Fig. 2(a)]. The temperature dependence of the static dielectric permittivity was fitted with Curie-Weiss law [Fig. 2(a)]

$$\varepsilon' = C_{p,f}/(|T - T_C|), \tag{1}$$

where $C_{p,f}$ are the Curie-Weiss constants in the paraelectric and ferroelectric phases, respectively, and T_C is the Curie temperature. Obtained parameters are $C_p = 8143$ K, $C_f = 41647$ K for $CuIn_{0.7}Cr_{0.3}P_2S_6$ and $C_p = 10\,555$ K, $C_f = 7737$ K for $CuIn_{0.8}Cr_{0.2}P_2S_6$. The ratio C_p/C_f is approximately 2 for both crystals; therefore, the phase transition is second order. The ratio $C_{p,f}/T_C$ is in the order 10; therefore, the observed phase transition is mainly order-disorder type. The dielectric dispersion is asymmetric for all crystals under study so that it cannot be described by the Cole-Cole formula. A more general approach must be used for the determination of the broad continuous distribution function of relaxation times $f(\tau)$ by solving the Fredholm integral equations,

$$\varepsilon'(\omega) = \varepsilon_\infty + \Delta\varepsilon \int_{-\infty}^{\infty} \frac{f(\tau)d(\ln\tau)}{1+\omega^2\tau^2}, \tag{2a}$$

$$\varepsilon''(\omega) = \Delta\varepsilon \int_{-\infty}^{\infty} \frac{\omega\tau f(\tau)d(\ln\tau)}{1+\omega^2\tau^2}, \tag{2b}$$

with the normalization condition

$$\int_{-\infty}^{\infty} f(\tau)d(\ln\tau) = 1. \tag{3}$$

The most general method for the solution is the Tikhonov regularization[16] method. The calculated distribution of relaxations times for $CuIn_{0.8}Cr_{0.2}P_2S_6$ is presented in Fig. 2(b). Broad and asymmetric distributions of relaxation times are observed in presented ferrielectrics. The longest limit of the $f(\tau)$ function was calculated [level 0.1 of the maximum $f(\tau)$ was chosen for definition of the limits] at various temperatures [Fig. 2(c)]. The temperature dependence of the longest relaxation times at low temperatures follows the Vogel-Fulcher law,

$$\tau = \tau_0 \exp\frac{E}{k(T - T_0)}. \tag{4}$$

The best-fitted parameters are $\tau_0 = 22.4$ ps, $E/k_B = 2083$ K, $T_0 = 15$ K for $Cu(In_{0.8}Cr_{0.2})P_2S_6$ and $\tau_0 = 1$ ps, $E/k_B = 2256$ K, $T_0 = 23$ K for $Cu(In_{0.7}Cr_{0.3})P_2S_6$.

B. Dipolar glass phase in mixed $Cu(In_xCr_{1-x})P_2S_6$ crystals

For $Cu(In_xCr_{1-x})P_2S_6$ crystals with $x = 0.4$–0.6 no anomaly in the static dielectric permittivity indicating a polar phase transition can be detected down to the lowest temperatures. The dielectric spectra of these crystals are very similar. As an example, the real and imaginary parts of the complex dielectric permittivity of $Cu(In_{0.5}Cr_{0.5})P_2S_6$ crystals are shown in Fig. 3 as functions of temperature at several frequencies. It is easy to see a broad dispersion of the complex

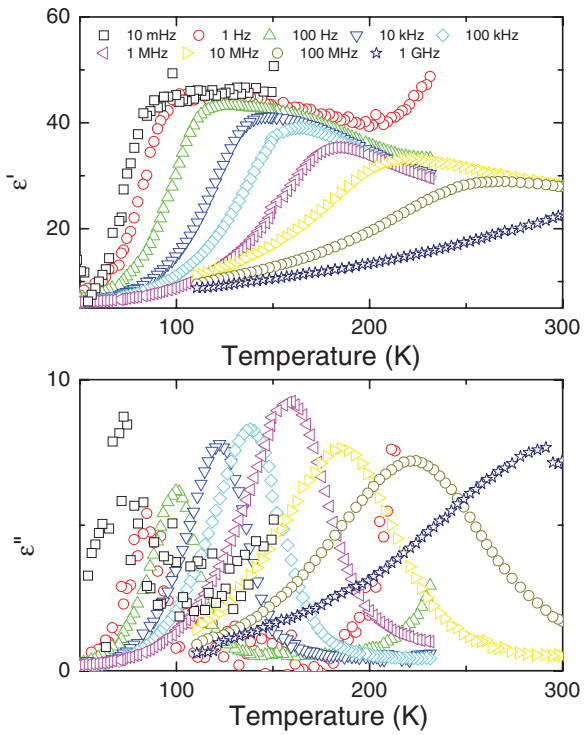

FIG. 3. (Color online) Temperature dependence of the complex dielectric permittivity of $CuIn_{0.5}Cr_{0.5}P_2S_6$ crystals measured at several frequencies.

dielectric permittivity starting from 260 K and extending to the lowest temperatures. The maximum of the real part of the dielectric permittivity shifts to higher temperatures with increasing frequencies together with the peak of the imaginary part in the whole frequency range. This is the main difference between the ferroelectric behavior observed in $Cu(In_{0.8}Cr_{0.2})P_2S_6$ (Fig. 1) where the ferroelectric phase transition temperature can be determined as the frequency-independent temperature of the maximum of the dielectric permittivity at low frequencies and the dipolar glass behavior in $Cu(In_{0.5}Cr_{0.5})P_2S_6$ (Fig. 3), where the peak temperature of the dielectric permittivity is frequency-dependent in the whole frequency range and does not indicate any phase transition temperature. This manifests the typical behavior of dipolar glasses. Broad and very asymmetric distributions of relaxation times are observed in both investigated dipolar glasses [Fig. 4(a)]. To get more insight into the nature of these distributions, they are fitted by a double well potential model.[17] We consider a copper ion moving in an asymmetric double well potential. The movement consists of fast oscillations in one of the minima with occasional thermally activated jumps between the minima. The jump probability is governed by the Boltzmann probability of overcoming the potential barrier between the minima. The relaxation time in such a system is given by[18]

$$\tau = \tau_0 \frac{\exp[E_b/k_B(T - T_0)]}{2\cosh(A/2k_BT)}. \tag{5}$$

The parameter A accounts for the asymmetry of the local potential produced by the mean field influence of all the other dipoles. We further consider that the asymmetry A and the potential barrier E_b of the local potential are randomly distributed around their mean values A_0 and E_{b0} according to the Gaussian law resulting in the distribution functions

$$f(E_b) = \frac{1}{\sqrt{2\pi}\sigma_{Eb}}\exp\left(-\frac{E_b - E_{b0}}{2\sigma_{Eb}^2}\right) \tag{6}$$

and

$$f(A) = \frac{1}{\sqrt{2\pi}\sigma_A}\exp\left(-\frac{A - A_0}{2\sigma_A^2}\right), \tag{7}$$

where σ_{Eb} and σ_A are the standard deviations of E_b and A, respectively, from their mean values. Thus the local polarization of the copper ions[18]

$$p = \tanh(A/2k_BT) \tag{8}$$

and the distribution function $w(p)$ of the local polarizations

$$w(p) = \frac{2k_BT}{\sqrt{2\pi}\sigma_A(1 - p^2)}\exp\left[-\frac{[\text{artanh}(p) - \text{artanh}(P)]^2}{2\sigma_A(2k_BT)^2}\right], \tag{9}$$

which transforms into the forms known for the random bond–random field (RBRF)[19] when substituting

$$\sigma_A = 2J\sqrt{q_{EA} + \Delta} \tag{10}$$

and

$$A_0 = 2J_0P. \tag{11}$$

Here, P is the average (macroscopic) polarization, J is the Gaussian variance and J_0 the average of the random interbond

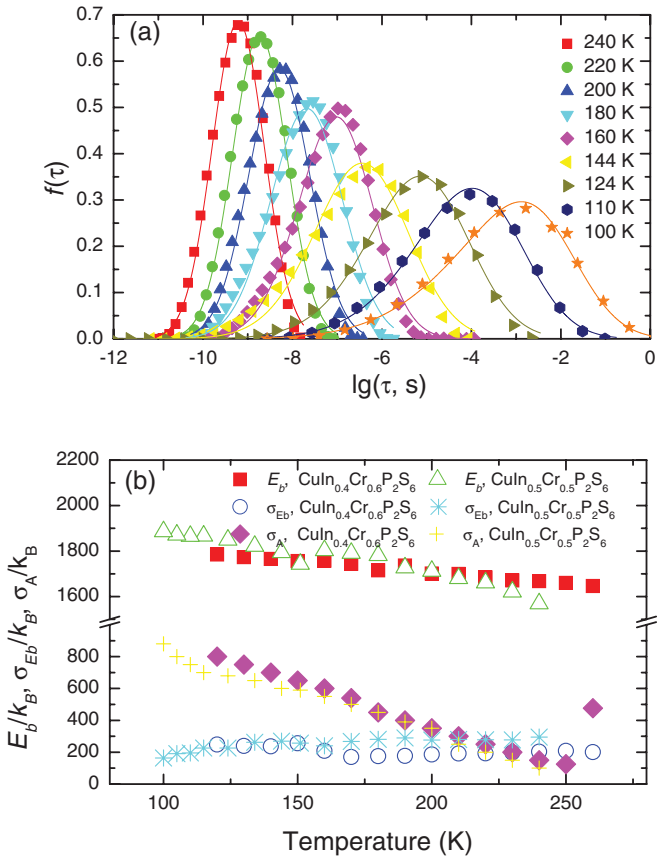

FIG. 4. (Color online) Distribution of relaxation times of $CuIn_{0.5}Cr_{0.5}P_2S_6$ at different temperatures (a) and temperature dependence of the mean values E_b, A and standard deviations σ_{Eb}, σ_A of mixed $CuIn_{0.5}Cr_{0.5}P_2S_6$ (open symbols) and $CuIn_{0.4}Cr_{0.6}P_2S_6$ crystals (solid symbols) (b).

coupling, Δ is the variance of the random local electric fields, and P the average (macroscopic) polarization. Fits with the experimentally obtained relaxation-time distributions were performed simultaneously using the same parameter set: $\tau_0 =$ 1 ps, $T_0 = 31$ K for $CuIn_{0.5}Cr_{0.5}P_2S_6$ and $\tau_0 = 0.98$ ps, $T_0 =$ 20 K for $CuIn_{0.4}Cr_{0.6}P_2S_6$. The result for $CuIn_{0.5}Cr_{0.5}P_2S_6$ is presented in Fig. 4(a) as solid lines. Other fit parameters are temperature dependent, as shown in Fig. 4(b). For the frozen copper ions, the average potential barrier height E_b is almost temperature independent. The potential barrier height and asymmetry distribution is very broad especially at low temperatures. The local polarisation distributions have been calculated from the double well potential parameters (Fig. 5). The temperature behavior of the local polarization distribution is very similar to that of other dipolar glasses, like DRADP.[20] It denotes that the dielectric dispersion in the $CuIn_xCr_{1-x}P_2S_6$ dipole glasses can be described by the RBRF model.[19] The Edwards-Anderson order parameter has been calculated from the local polarization distribution

$$q_{EA} = \int p^2 w(p) dp. \tag{12}$$

It is an almost linear function of temperature and does not indicate any anomaly (Fig. 6). The macroscopic polarization

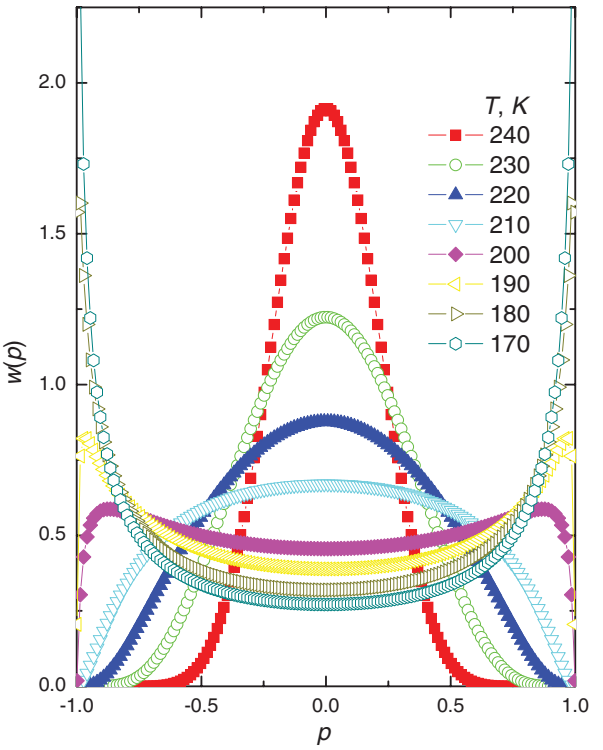

FIG. 5. (Color online) Distribution of local polarization of $CuIn_{0.5}Cr_{0.5}P_2S_6$ crystals.

can also be calculated,

$$P = \int p w(p) dp. \tag{13}$$

The calculated value is vanishing, as it should be for disordered structures.

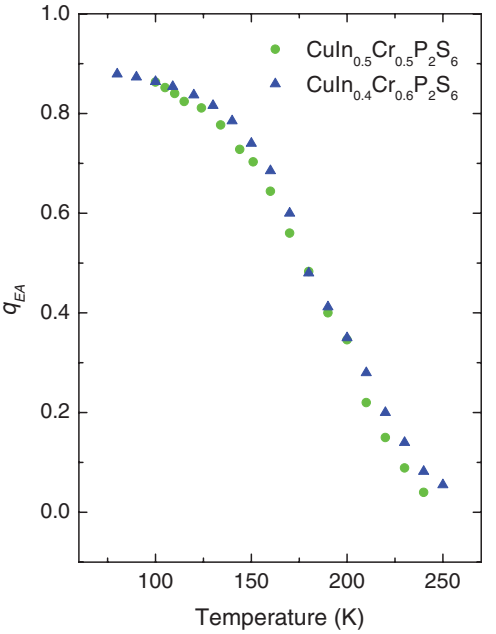

FIG. 6. (Color online) Edwards-Anderson order parameter of $CuIn_{0.5}Cr_{0.5}P_2S_6$ and $CuIn_{0.4}Cr_{0.6}P_2S_6$ crystals.

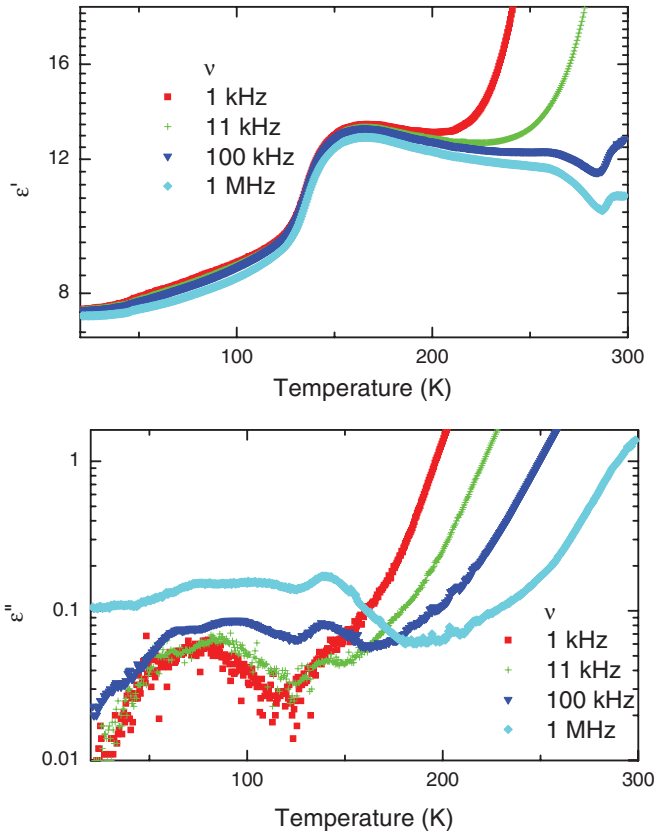

FIG. 7. (Color online) Temperature dependence of the complex dielectric permittivity of $CuIn_{0.1}Cr_{0.9}P_2S_6$ crystals measured at several frequencies.

C. Antiferroelectric phase transition region

The phase transition in $CuIn_{0.1}Cr_{0.9}P_2S_6$ is accompanied by a steplike dielectric anomaly (Fig. 7). The width of the step is approximately 20 K. Taking the temperature, corresponding to the peak point of the step in the real part of dielectric permittivity as the temperature of the phase transition, it was found that $T_c = 167$ K. A similar dielectric behavior is observed in $CuCrP_2S_6$ except for a narrower step in the temperature dependence of the dielectric permittivity. Here it is 5 K. The peak point of the step lies approximately at 170 K. It is close to that observed in Refs. 11 and 9. There is a noticeable shift of the antiferroelectric phase transition temperature due to the substitution of In by Cr in the mixed $CuIn_xCr_{1-x}P_2S_6$ antiferroelectrics. The antiferroelectric phase transition temperature further decreases by increasing chromium concentration and for $CuIn_{0.2}Cr_{0.8}P_2S_6$ it reaches a value of 125 K.[14] As can be seen from Fig. 7, at temperatures $T > 200$ K the dielectric permittivity shows a sharp increase with temperature and reveals a pronounced frequency dependence. Obviously hopping conductivity causes this dielectric behavior, similarly as in pure $CuCrP_2S_6$.[12]

While analyzing the sample from low temperatures, the permittivity rises slowly between 30 and 136 K for $CuIn_{0.1}Cr_{0.9}P_2S_6$ and 150 K for $CuCrP_2S_6$, after which it increases abruptly and then slightly, while at 167 K for $CuIn_{0.1}Cr_{0.9}P_2S_6$ and 170 K for $CuCrP_2S_6$ it starts decreasing. The T width of this dielectric anomaly and the slope changes just below 167 K ($CuIn_{0.1}Cr_{0.9}P_2S_6$) and 170 K ($CuCrP_2S_6$) agree with a hypothesis of a slowly evolving short-range dipole order.[11] Knowing that the copper dipole configuration is antipolar at $T < 150$ K, we infer from the relatively continuous decrease at 125 K ($CuIn_{0.1}Cr_{0.9}P_2S_6$) and 150 K ($CuCrP_2S_6$) that the intermediate phase is quasi-antipolar (or incommensurate). It was found that the dielectric permittivity follows the Curie-Weiss law. The ratio of $C_p/C_{af} \gg 2$ hints at a first-order antiferroelectric phase transition in the crystals.

It should be mentioned that the dielectric loss in $CuCrP_2S_6$ does not show any remarkable anomalous behavior either in the vicinity of the phase transition or in the antiferroelectric phase at lower temperatures. In contrast, in $CuIn_{0.1}Cr_{0.9}P_2S_6$ below the antiferroelectric phase transition a broad dielectric relaxation is observed (Fig. 7). A similar dielectric behavior is also observed in $CuIn_{0.2}Cr_{0.8}P_2S_6$.[14] The dielectric relaxation is obviously caused by antiferroelectric domain dynamics. The similar dielectric relaxation caused by antiferroelectric domain dynamics has already been observed in $CuBiP_2Se_6$ crystals.[21] The zero value of the freezing temperature observed in $CuIn_{0.2}Cr_{0.8}P_2S_6$ by fitting the frequency of loss peaks is also very similar to the low value of the freezing temperature of the longest relaxation time in $CuBiP_2Se_6$ (2 K).[14,21]

These features refer also very probably to independent Debye-type relaxation processes.[14] At higher dilutions, $x > 0.3$, a hierarchical dipolar glassy polydispersivity arises, which

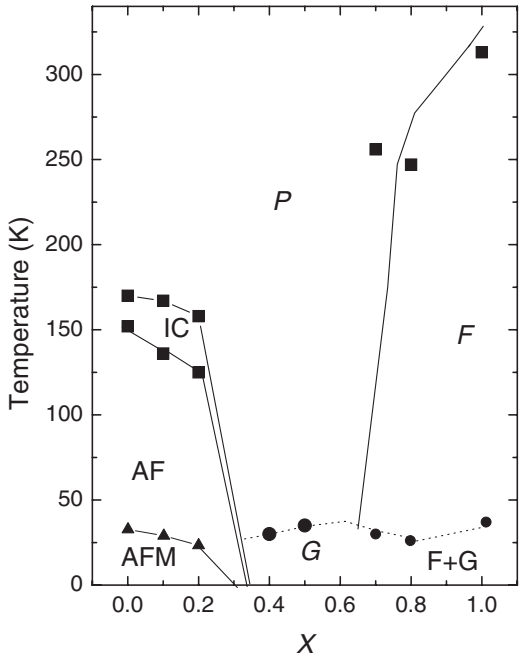

FIG. 8. Phase diagram of $CuIn_xCr_{1-x}P_2S_6$ crystals: P, paraelectric phase; IC, incommensurate phase; AF, antiferroelectric phase; AFM, antiferomagnetic phase; G, dipolar glass phase; F, ferrielectric; $F + G$, coexistence of ferrielectric and dipolar glasses. Squares are obtained from the static dielectric permittivity maximum, circles from Vogel-Fulcher fit of the longest relaxation time, and triangles from Ref. 14. The solid lines are a guide for eyes.

has been discussed above and elsewhere.[22] Tentatively, we consider this behavior to follow the rules of percolation theory. While the antiferroelectric backbone phase is nearly unperturbed by the occurrence of impurity-induced relaxing dipolar clusters, the latter require a critical concentration, $x_{cr} \approx 0.3$, in order to form a coherent glassy subsystem. We propose this to be based on frustrated dipolar interaction similar to that occurring in the magnetic spin cluster glass, which coexists with the dilute antiferromagnetic "backbone" phase in $Pb(Fe_{0.5}Nb_{0.5})O_3$.[23]

D. Phase diagram

The phase diagram of $CuIn_xCr_{1-x}P_2S_6$ solid solutions obtained from our dielectric results is shown in Fig. 8. Coexistence of ferroelectric ordering with a dipolar glass phase in $CuIn_xCr_{1-x}P_2S_6$ is present at $x \geqslant 0.7$. On the other side of the phase diagram for $x \leqslant 0.2$ the antiferroelectric phase transition occurs. By decreasing the concentration x, the antiferroelectric phase transition temperature increases. In the intermediate concentration range, $0.4 \leqslant x \leqslant 0.6$, a dipolar glass phase is observed.

IV. CONCLUSIONS

Dilute solid solutions of $CuIn_xCr_{1-x}P_2S_6$ reveal various long-range ordered polar (ferri- and antiferrielectric) and magnetic phases (antiferromagnetic) as shown in the phase diagram of Fig. 8. Two types of single phase ferroic behavior are observed. While at high Cr^{3+} concentrations, $1 - x > 0.7$, the system is antiferroelectric-antiferromagnetic at low temperatures, large In^{3+} concentrations, $x \geqslant 0.7$, favor the coexistence of ferrielectric long-range order with a dipolar cluster glass. It remains an open question if the dipolar glass, which dominates at intermediate concentrations, $0.4 \leqslant x \leqslant 0.6$, might coexist with a generic spin glass.

ACKNOWLEDGMENTS

We wish to acknowledge the support of the Research Council of Lithuania funding this work according to the project "Postdoctoral Fellowship Implementation in Lithuania".

*andrius.dziaugys@ff.vu.lt

†Present address: Institute for Materials Science, Universität Duisburg-Essen, D-45141, Essen, Germany.

[1] K. Binder and J. D. Reger, Adv. Phys. **41**, 547 (1992).

[2] R. Blinc, J. Dolinsek, R. Pirc, B. Tadic, B. Zalar, R. Kind, and O. Liechti, Phys. Rev. Lett. **63**, 2248 (1989).

[3] H. Bauch, G. Völkel, R. Böttcher, A. Pöppl, H. Schäfer, J. Banys, and A. Klöpperpieper, Phys. Rev. B **54**, 9162 (1996).

[4] J. Banys, J. Macutkevic, S. Lapinskas, C. Klimm, G. Völkel, and A. Klöpperpieper, Phys. Rev. B **73**, 144202 (2006).

[5] V. Maisonneuve, V. B. Cajipe, A. Simon, R. Von Der Muhll, and J. Ravez, Phys. Rev. B **56**, 10860 (1997).

[6] A. Simon, J. Ravez, V. Maisonneuve, C. Payen, and V. B. Cajipe, Chem. Mater. **6**, 1575 (1994).

[7] X. Bourdon, A. R. Grimmer, and V. B. Cajipe, Chem. Mater. **11**, 2680 (1999).

[8] Yu. M. Vysochanskii, V. A. Stephanovich, A. A. Molnar, V. B. Cajipe, and X. Bourdon, Phys. Rev. B **58**, 9119 (1998).

[9] K. Moriya, N. Kariya, A. Inaba, T. Matsuo, I. Pritz, and Yu. M. Vysochanskii, Solid State Commun. **136**, 173 (2005).

[10] V. Maisonneuve, C. Payen, and V. B. Cajipe, J. Solid State Chem. **116**, 208 (1995).

[11] V. B. Cajipe, J. Ravez, V. Maisonneuve, A. Simon, C. Payen, R. Von Der Muhll, and J. E. Fischer, Ferroelectrics **185**, 135 (1996).

[12] V. Maisonneuve, J. M. Reau, M. Dong, V. B. Cajipe, C. Payen, and J. Ravez, Ferroelectrics **196**, 257 (1997).

[13] J. Banys, J. Macutkevic, V. Samulionis, A. Brilingas, and Yu. Vysochanskii, Phase Transit. **77**, 345 (2004).

[14] W. Kleemann, V. V. Shvartsman, P. Borisov, J. Banys, and Yu. M. Vysochanskii, Phys. Rev. B **84**, 094411 (2011).

[15] A. Dziaugys, J. Banys, J. Macutkevic, R. Sobiestianskas, and Yu. Vysochanskii, Phys. Status Solidi A **207**, 1960 (2010).

[16] A. N. Tikhonov and V. Y. Arsenin, *Solution of Ill-posed Problems* (Wiley, New York, 1977).

[17] J. Banys, S. Lapinskas, A. Kajokas, A. Matulis, C. Klimm, G. Volkel, and A. Klopperpieper, Phys. Rev. B **66**, 144113 (2002).

[18] J. Dolinsek, D. Arcon, B. Zalar, R. Pirc, R. Blinc, and R. Kind, Phys. Rev. B **54**, R6811 (1996).

[19] R. Pirc, B. Tadic, and R. Blinc, Phys. Rev. B **36**, 8607 (1987).

[20] J. Banys, J. Macutkevic, S. Lapinskas, R. Pirc, Z. Kutnjak, and R. Blinc, J. Appl. Phys. **109**, 114101 (2011).

[21] A. Dziaugys, J. Banys, J. Macutkevic, Yu. Vysochanskii, I. Pritz, and M. Gurzan, Phase Transit. **84**, 147 (2011).

[22] A. Dziaugys, J. Banys, V. Samulionis, J. Macutkevic, Y. Vysochanskii, V. V. Shvartsman, and W. Kleemann, in *Ferroelectrics, 3*, edited by M. Lallart (InTech Open Access, Rijeka, 2011), p. 153.

[23] W. Kleemann, V. V. Shvartsman, P. Borisov, and A. Kania, Phys. Rev. Lett. **105**, 257202 (2010).